Egypt. J. Solids, Vol.(44) (2022)

Impact of pre-torsional deformation and nanoparticles addition on the mechanical behavior of Sn-based soft solder alloy

M. Sobhy*

Department of Physics, Faculty of Education, Ain Shams University, P.O. Box 5101, Heliopolis 11771, Roxy, Cairo, Egypt

Receive Date:18 September 2022; Revise Date: 30 September 2022 ;Accepted Date: 5 October 2022 ; Publish *Date:* 6 October 2022.

Abstract

This research aimed to study the effect of pre-deformation by torsion and the addition of ZnO nanoparticles on the microstructure and tensile behavior of Sn-based soft solder alloys. The used alloys are Sn-3Ag-0.7Cu (SAC307) and Sn-3Ag-0.7Cu doped with 0.3wt%ZnO nanoparticles SACZ3(307). Pre-deformation increases the dislocation density consequently the lattice strain is increased. Applying pre-torsional deformation before the tensile test resulted in the enhancement of the mechanical properties $\sigma_{y0.2}$, σ_f and χ_p for both SAC (307) and composite solders at different working temperatures. These changes in mechanical properties depend on the internal structure of both solders since deformation generates an excess of mixed defects. Also, the dispersed intermetallic compounds (IMCs) particles hinder the motion of dislocations. This study includes new and novel results about the behavior of fracture strain ε_f with deformation at different working temperatures. According to the obtained activation energy Q values, the dislocation-IMCs interaction is the deformation mechanism taking place in both alloys.

E-mail address: miladsobhy@edu.asu.edu.eg (M. Sobhy*).

Keywords:SACZ3(307); Stress-Strain; degree of deformation; cold work; nanoparticles; work hardening.

Introduction

Solders are essential materials in the electronic industry since they provide a good electrical connection with a suitable mechanical response between the substrate and the integrated circuit devices [1]. Previously, Sn–Pb solder alloy has been used in electronic packaging due to its superior wettability, moderate melting temperature (183 °C), good performance, and low price. In 2006, the international legislations forestall the exploitation of lead within industrial production owing to its toxicological severe considerations to the environment [2,3]. Recently, the development of Sn-free solders with suitable mechanical properties has attracted much attention to avoid the toxicity of conventional lead-based solders [4,5].

Sn-Ag-based alloys are examples of these lead-free solders, but their mechanical properties need to be enhanced. In this direction, the microstructure is to be changed by the addition of small amounts of some elements like Cu, Zn, Bi, and Sb [6-12]. Many researchers chose rare earth, Ge, Ni, Ga, Co, and In. Furthermore, a novel way was used to improve solder properties by the addition of nano-oxide materials such as Al_2O_3, ZnO and SiC that acts as pinners for grain boundary migration [4,5,13,14]. The addition of the fourth elements; Fe, Ti,Co, Mn, and Ni on the microstructure and mechanical properties of Sn-Ag-Cu solder was studied by Kim and co-workers [15]. They found that all quaternary alloys from third IMCs in addition to fine Ag_3Sn and Cu_6Sn_5, exhibit improved solder structure. All quaternary bulk alloys exhibit large tensile strength. Fawzy et al [5], studied the effect of adding ZnO nanoparticles to SAC355 solder and found that it significantly

suppressed the formation of Ag_3Sn and Cu_6Sn_5 intermetallic compound particles and restricted their volume fraction. Moreover, these nanoparticles controlled the growth of β-Sn grains in the matrix and reduced the grain size with the enhancement of the tensile creep resistance.

Generally, cold working enhances the mechanical properties of the material. So, it was thought to think about deformation in the process of refining β-Sn grains to improve the microstructure of Sn-Ag-Cu solder alloy. It is worthy to mention that pre-deformation can control grain growth. It can be predicted that this process of deformation may improve the microstructure of the solder besides other factors and enhance the mechanical properties.

It is observed that the literature is depleted from the effect of torsional deformation on the mechanical behavior of Sn-based solder alloys, so it seemed to be a good benefit to consider this work as an original and novel direction in this field.

2. Experimental Procedures

The alloy used in this work SAC(307) was prepared from 99.99% pure Ag, Sn, and Cu ingots. The composite solder alloy SACZ3(307) was made by physically combining 0.3 wt.% ZnO particles into prepared conventional SAC(307) alloy. Homogenization was attained by two times remelting at 623 K for 2.5 hours in a vacuum furnace and leaving the melt to cool in the air. The obtained alloys in the form of bars were cold-drawn into wires of 0.7 mm diameter. For, metallographic observations, a sheet of 0.5 mm thick is obtained by rolling a portion of each alloy. A solution of 80 % glycerine, 10% acetic acid and10% nitric acid for 20 sec is used as an etchant.

The surface features of the two solders were examined by an optical microscope(OM)[type Kyowa Microscope].Scanning electron microscopy (FESEM) SU8000 series equipped with EDX energy dispersive x-ray and X-ray diffractometer [Philips diffractometer (40 kV)] with atomic number 29 K_{σ} radiation(λ = 0.15406 nm) was used .XRD patterns were recorded within the 2θ range 27–82°. Tensile tests were performed on samples with a gauge length of 50 mm, by stretching until fracture, using a modified locally made tensile testing machine described elsewhere [16]. Measurements

are carried out at different degrees of deformation Θ ranging from Θ = 0 up to 80% [Θ = N/N_f]where N is the number of turns twists given to the specimen and N_f is the number of turns twists necessary to fracture it at different working in the range from R.T up to 373 K. Heating the wires was applied during the tensile test. The temperature was measured with an accuracy of ±1K. In order to stabilize the microstructure of the tested specimens, they were kept for one month at R.T to remove the defects formed during specimen processing.

3. Experimental Results and Discussion

3.1 Structure identification

A (TEM) image for the Zinc oxide nanoparticles was used in this investigation. The average size of 40 nm for the ZnO nanoparticle was deduced (see figure1).

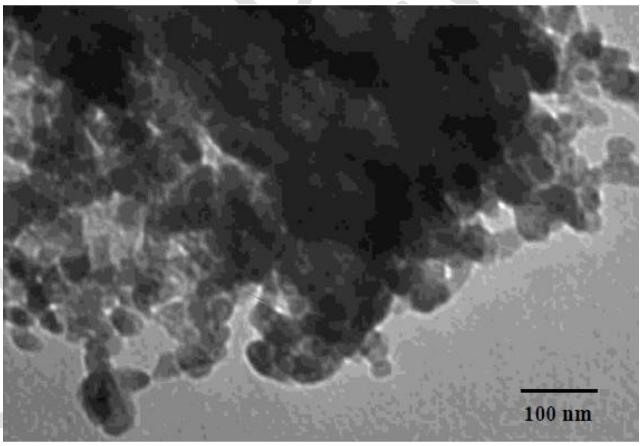

Fig. 1. TEM for ZnO nano-particles.

Figure 2(a,b) is an optical micrograph showing the microstructure of SAC307 and SACZ3(307). Figure 2(a) shows the irregular coarsened grain in the SAC307 alloy. In Figure 2(b), a very clear change in β-Sn a refined grain size are observed with the addition of ZnO nanoparticles. The above changes in microstructure is be explained by

the effect of the IMCs that formed during the solidification process and their segregation on grain boundaries leading to hindering their motion.

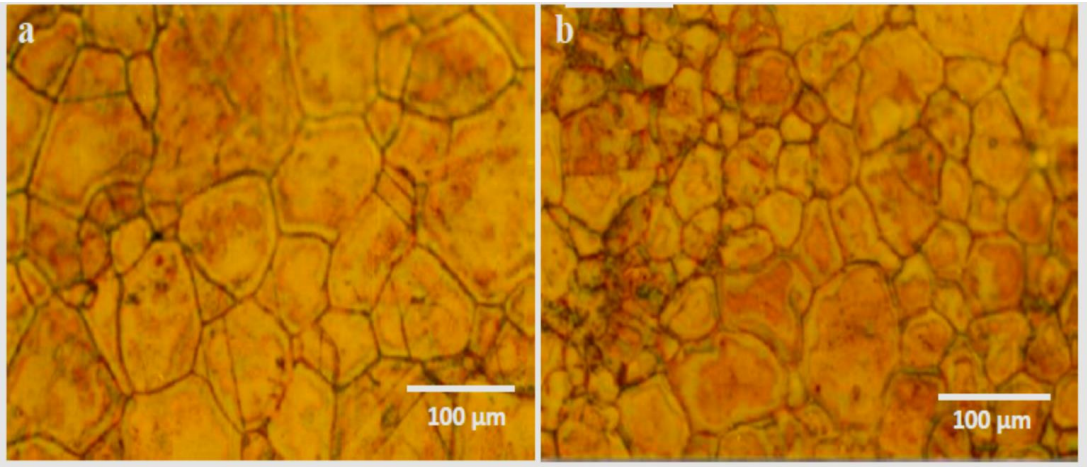

Fig. 2. Metallographic micrographs of (a) SAC307, (b) SACZ3(307) solder alloys.

EDS was used to determine the elemental composition of IMC particles, as presented in Figure 3 (a,b) in which Ag_3Sn, Cu_6Sn_5 are identified. These particles are distributed and vary differently in size according to the degree of deformation.

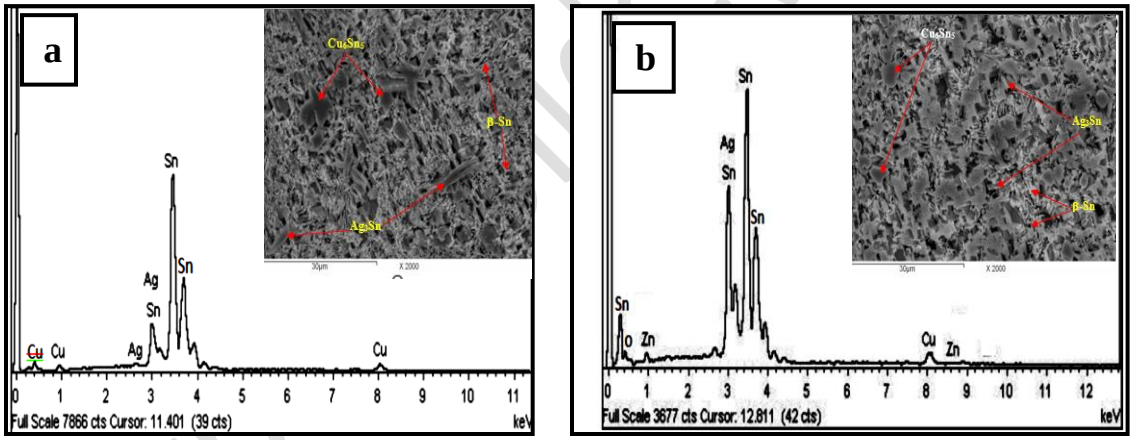

Fig. 3. (a)SEM micrographs and inset EDS for: a-SAC307 b- SACZ3(307) solder alloys illustrating the variation of IMC particle size

EDX of both SAC(307) and SACZ3(307) lead-free soft solder alloys exhibited only peaks of three types of phases: Cu_6Sn_5, β-Sn, and Ag_3Sn as shown in figure 4(a,b).

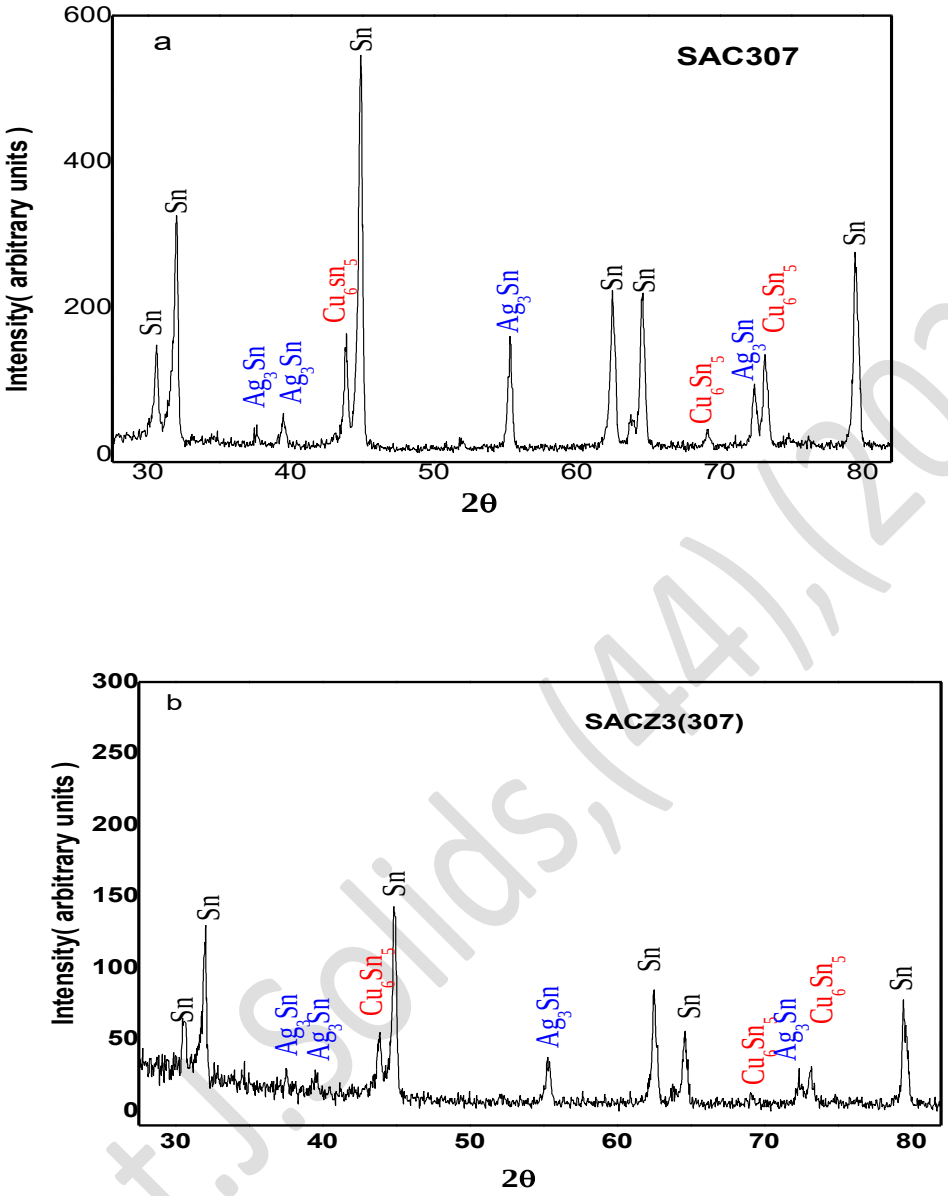

Fig. 4. XRD pattern of (a) SAC307, (b) SACZ3(307) solder alloys

The as-received microstructure of Sn-3Ag-0.7Cu alloy is shown in figure 5 (a). It consists of primary Sn grains surrounded by Ag_3Sn and Cu_6Sn_5. It is also observed that somewhat larger Ag_3Sn precipitates may form. The SACZ3(307) solder alloy shows fine precipitates figure 5(b).

Egypt. J. Solids, Vol.(44) (2022)

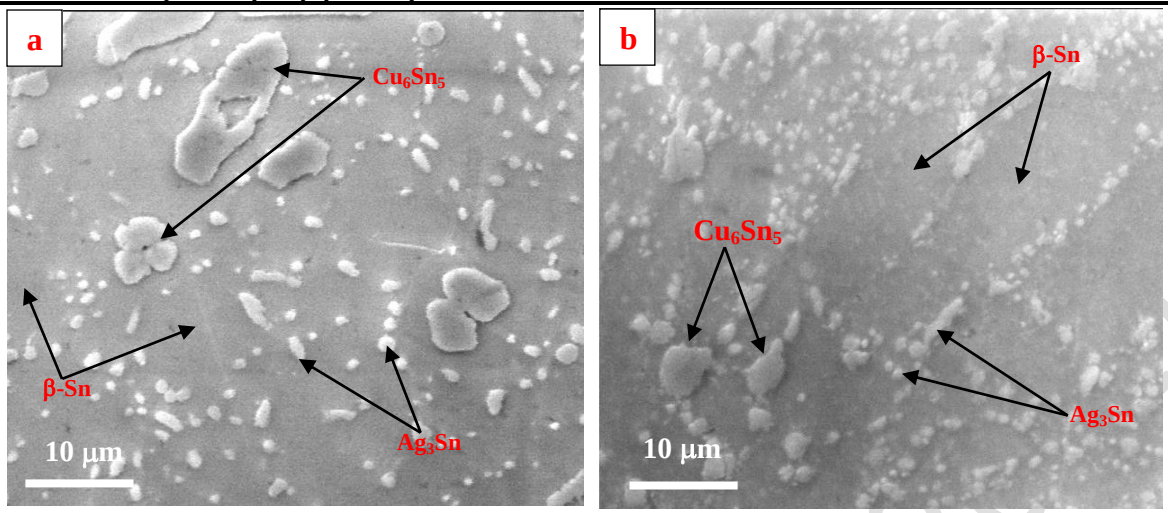

Fig. 5. SEM micrographs showing the IMCs in(a) SAC307 solder and (b) SACZ3(307) solder alloys.

Thus, it may be summarized that the addition of nanosized particles suppresses and controls ,the β-Sn dendrites and uniform dispersion of the Sn-rich matrix leading to a fine network microstructure as illustrated in figure 5(b). This improves the mechanical properties of the solder [13,17-22].

3.2 Tensile response

Cold working is an important industrial process that is used to harden metals and alloys. Plastic torsion of the test wires was affected using the tensile testing machine previously described [16]. The degree of pre-deformation by torsion $\Theta = N/N_f$, N the number of turns twist given to the specimen and N_f is the number of turns twist required to fracture the specimen at the same condition.

Typical sets of (σ - ε) curves of both plain and composite solders were carried out at different degrees of torsional deformation Θ (= 0, 20, 40, 60 and 80%) and tested at working temperatures ranging from 298 to 373K. Figure (6) shows that the curves of SACZ3(307) alloy have higher values than those of nanoparticle-free solder at all test

conditions. This can be explained by the variation in the microstructures of plain and composite solders as shown in figure 5(a,b)which is considered good evidence that dispersion strengthening due to the refinement and uniform distribution of the IMCs are the main cause of the observed increase in hardenability of composite solder.

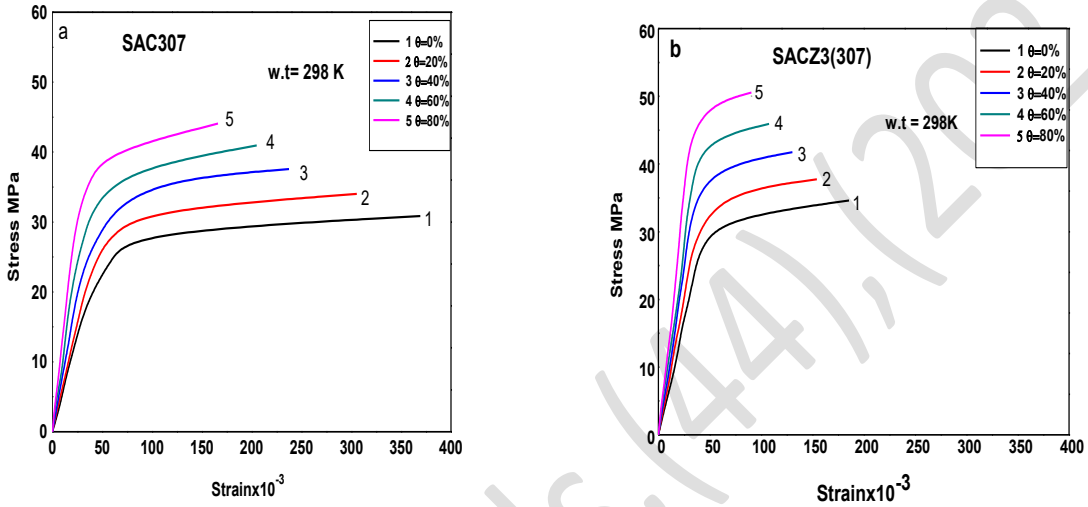

Fig. 6. Representative (σ - **ε**) curves for samples differently deformed at 298 for:

(a) SAC307 , (b) SACZ3(307)

Figure7: illustrates a set of (σ - **ε**) curves for the two alloys, strained with Θ = 40% at different working temperatures ranging from 298 to 398 K .

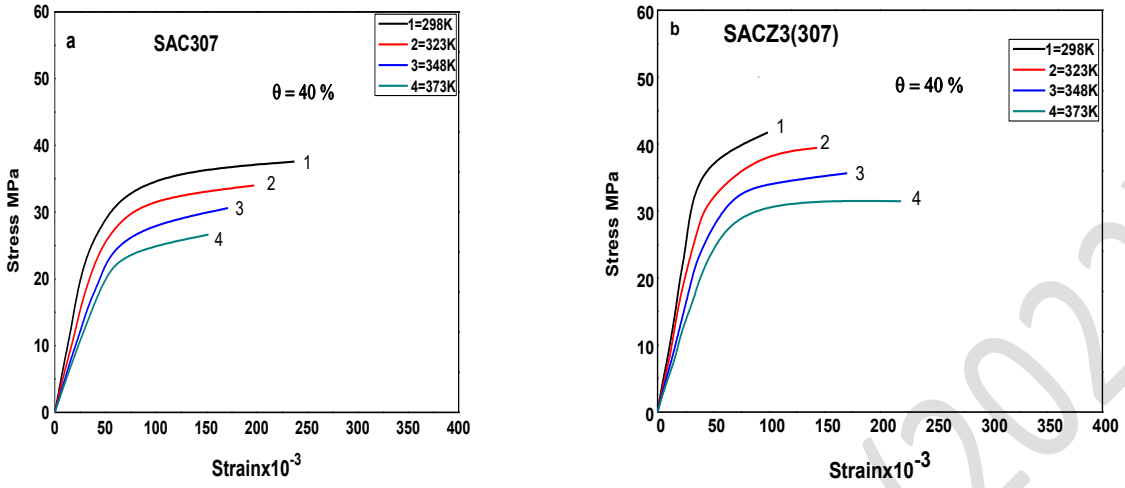

Fig. 7. Representative (σ - **ε**) curves for samples differently tested temperature at Θ=40% for:

(a) SAC307 , (b) SACZ3(307)

Generally, it can be concluded from Figures6,7 that stress-strain relations are sensitive to both degrees of deformation Θ and working temperature T. Offset stress $\boldsymbol{\sigma}_{y0.2}$, fracture stress $\boldsymbol{\sigma}_f$ and fracture strain $\boldsymbol{\varepsilon}_f$ for both plain and doped alloys as a function of **Θ** at different working temperatures are presented in Figures 8, 9 and 10 respectively. From these figures, both $\boldsymbol{\sigma}_{y0.2}$ and $\boldsymbol{\sigma}_f$ increased with increasing degree of deformation **Θ**, while they decreased with increasing the working temperature. With respect to the fracture strain $\boldsymbol{\varepsilon}_f$, it was found that it decreases with increasing degree of deformation for both solders, but the effect of working temperature on $\boldsymbol{\varepsilon}_f$ was surprising since it decreases with increasing temperature in the plain solder while it increases with increasing temperature in ZnO doped solder. Such strengthening effects can be explained as follows: most metals and solder alloys undergo simultaneous work hardening and dynamic recovery [23]. Strain-hardening and recovery have opposite effects on the mechanical characteristics of metals and alloys, with the former they harden and softening with the latter. The presented (σ - **ε**) curves in

this work appear to emphasize the combination of both mechanisms. The increase in hardenability is rendered to the increase in the density of the dislocation with increasing the degree of deformation while increasing the working temperature results in dislocation annihilation leading to softening at a constant deformation level, dynamic recovery has more effect on ($\boldsymbol{\sigma_{y0.2}}$ and $\boldsymbol{\sigma_f}$) than strain- hardening, which results in decreasing stress level. On the contrary, when the deformation level increases in the tensile test at a constant temperature, the effect of strain-hardening becomes predominant and results in rising $\boldsymbol{\sigma_{y0.2}}$ and $\boldsymbol{\sigma_f}$. Therefore, deformation and temperature have evident effects on this solder. The addition of ZnO nanoparticles resulted in increasing the hardenability of SAC solder, which may be attributed to the refinement of the IMCs Ag_3Sn, Cu_6Sn_5 leading to hindering the dislocation motion by their pinning action at all test conditions (Ѳ,T).

Figure 10(a,b) shows that at all working temperatures, $\boldsymbol{\varepsilon_f}$ in both alloys decreases with increasing degree of deformation. The effect of working temperature was found different, in both ZnO-free and composite alloys. Figure10 (a) at any value of Ѳ, $\boldsymbol{\varepsilon_f}$ decreased with T, while from fig10(b) it increased. This contradiction of $\boldsymbol{\varepsilon_f}$ behavior with working temperature may be explained as follows: The IMCs formed in SAC307 solder are loaded on the moving dislocations. The heat energy given to the sample by raising the working temperature cannot detach these particles, thus the dislocations can't move for long distances and the sample fractures faster indicating less fracture strain . On the contrary and in SACZ3(307) solder the IMCs are very fine and pin the moving dislocations in many places. Raising the working temperature can easily detach these particles and the dislocations can move easier leading to an increase in $\boldsymbol{\varepsilon_f}$ with increasing working temperature. This explanation may account for $\boldsymbol{\varepsilon_f}$ behavior with increasing working temperature in SACZ3(307) alloy.

Egypt. J. Solids, Vol.(44) (2022)

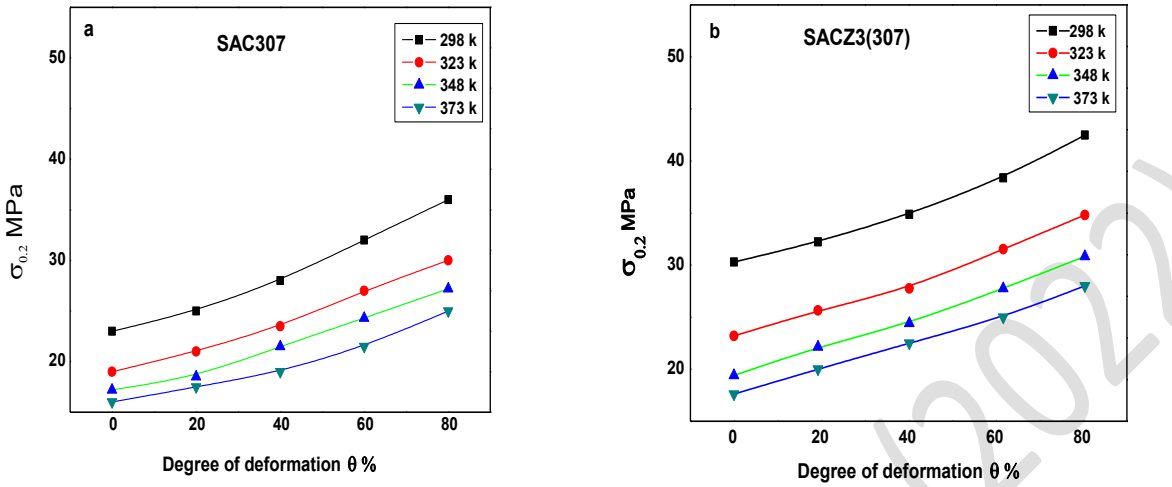

Fig. 8. Offset stress ($\sigma_{y0.2}$) as a function of torsional deformation **Θ** for (a)SAC307 and (b) SACZ3(307) at different working temperatures as indicated.

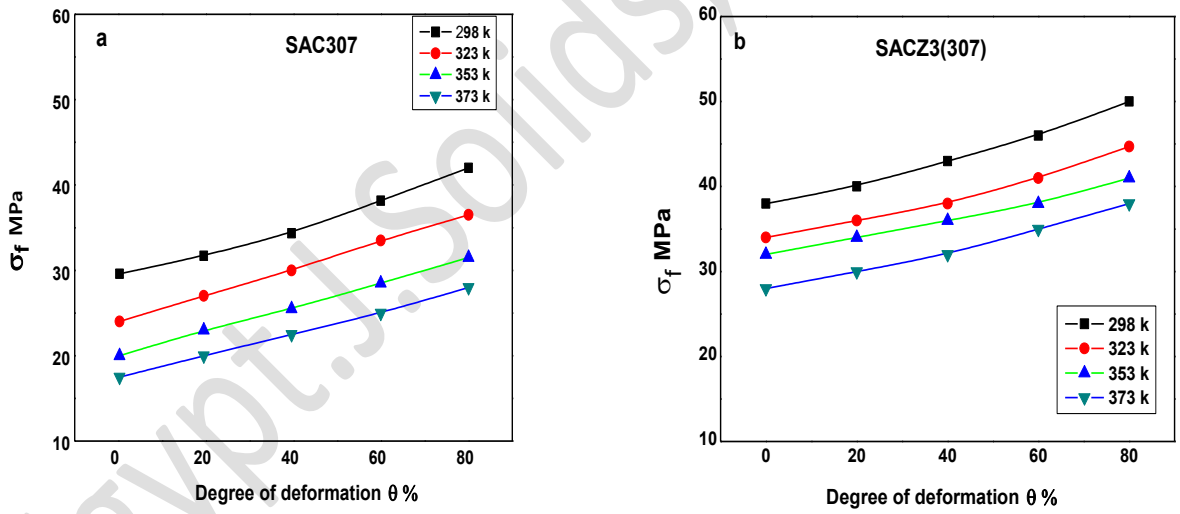

Fig. 9. Fracture stress (σ_f) as a function of torsional deformation **Θ** for (a) SAC307 and (b) SACZ3(307) at different working temperatures as indicated

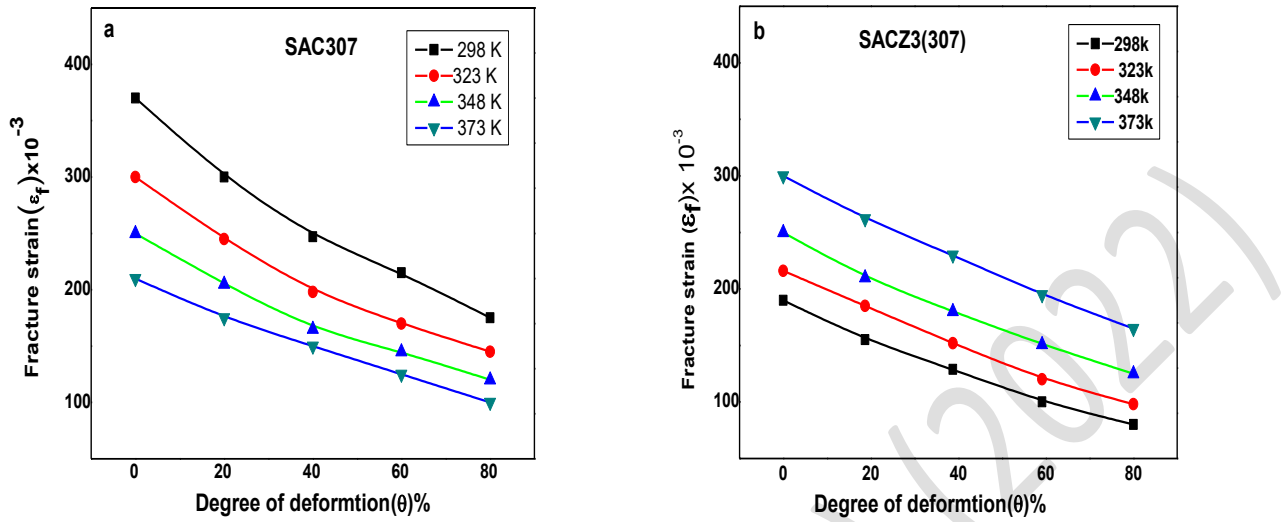

Fig. 10. Fracture strain(ε_{f}) as a function of torsional deformation **Θ** for (a)SAC307 and (b) SACZ3(307) at different working temperatures as indicated.

3. 3 Work hardening coefficient χ_p

The (σ - **ε**) curves of the alloys under consideration showed a parabolic relation past yield point. This implied the calculation of the work hardening coefficient $\chi_p=(\frac{\partial\sigma^2}{\partial\varepsilon})_T$ [16] as a function of **Θ** as shown in figure11(a,b) for SAC and composite respectively. For both solders, χ_p increases with increasing the degree of deformation and/or decreasing the working temperature. The addition of nano-sized ZnO particles is observed to increase the values of χ_p at all test conditions (working temperatures and degree of deformation).

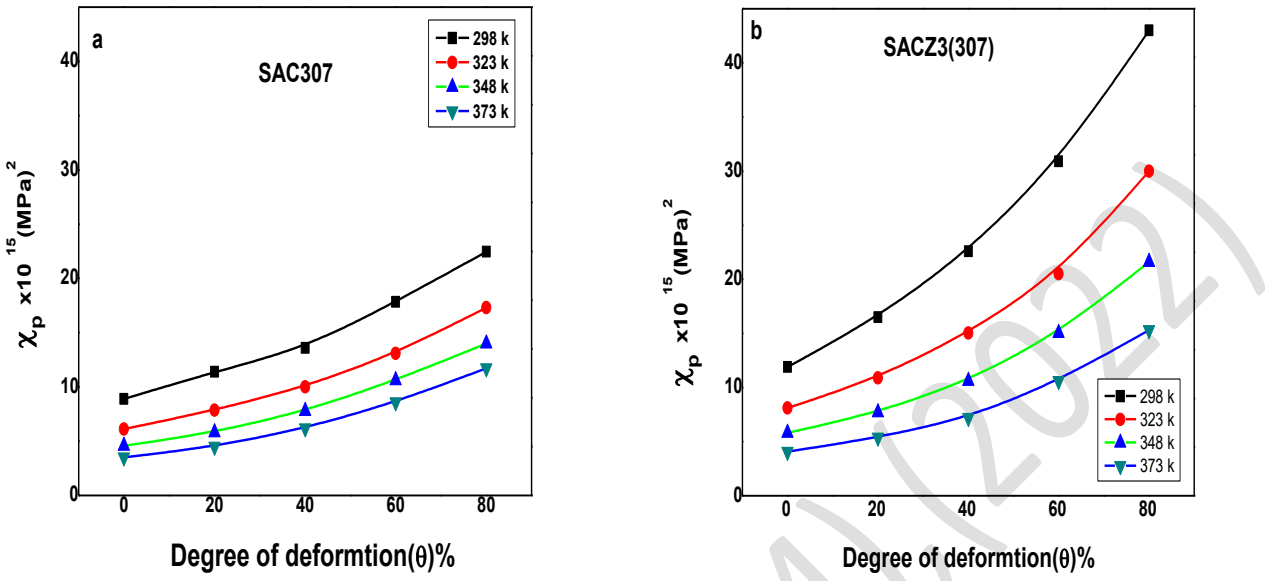

Fig. 11. Work hardening coefficient (χ_p) as a function **Θ** for (a)SAC307 and (b) SACZ3(307) at different working temperatures as indicated.

The parabolic work-hardening coefficient χ_p and slip distance L are related by: $\chi_p = G^2b / 2\pi^2 L$[24]. where b - Berger's vector, G - shear modulus. This relation was attributed to the formation of dislocation pile-ups against obstacles such as grain boundaries.

From the above relation, the slip distance L is calculated and its dependence on the degree of deformation **(Θ)** is illustrated in Figure12(a,b) for both alloys. It is obvious from Figure 12 that the slip distance L decreased with increasing plastic torsion deformation which is in contrast with the behavior of χ_p. This means that at a certain degree of deformation, the material of the highest work-hardening coefficient χ_p has the lowest slip distance L travelled by a moving dislocation and vice versa.

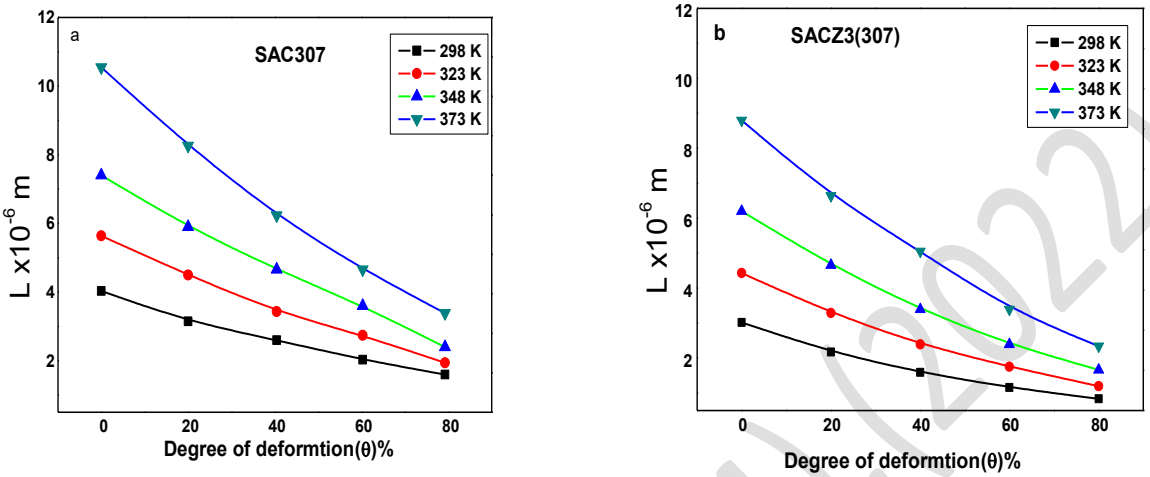

Fig. 12. Slip distance (L) as a function of torsional deformation **Θ** for (a)SAC307 and (b) SACZ3(307) at different working temperatures as indicated.

The decrease in χ_p with increasing working temperature illustrated in Figure11(a,b) could be explained as follows: dislocations easily overcome obstacles when thermal agitation is increased. Thus, L will be increased [25], leading to a decrease in χ_p. The values of χ_p of the SACZ3(307) solder showed higher values compared with those of plain solder at all working temperatures.

The observed increase in χ_p by increasing **Θ (**see Figure11) and the decrease of L of the moving dislocation observed in Figure 12, may be explained in terms of the interaction between these developed dislocation networks and present lattice imperfections [26] which may: i- stabilize the high energy configuration of dislocation, ii- retard the arrangement of dislocations necessary for the formation of large angle boundaries, iii- retard the migration of such boundaries once formed. This is consistent

with Figure 4(a,b) which presents a decrease in the grain sizes of the β-Sn matrix of the SACZ3(307) solder compared with those in the SAC307 plain solder alloy.

Activation energy

The activation energy Q of the deformation process is calculated from the variation of the work-hardening coefficient χ_p with the working temperature T, according to an Arrhenius type equation of the form : χ_p= const. exp$\left[\frac{Q}{K_B T}\right]$ [27] where K_B is the Boltzmann constant and T is the absolute working temperature. The Q value of both alloys was calculated by plotting lnχ_p versus 1000/T as shown in Figure 13(a,b).

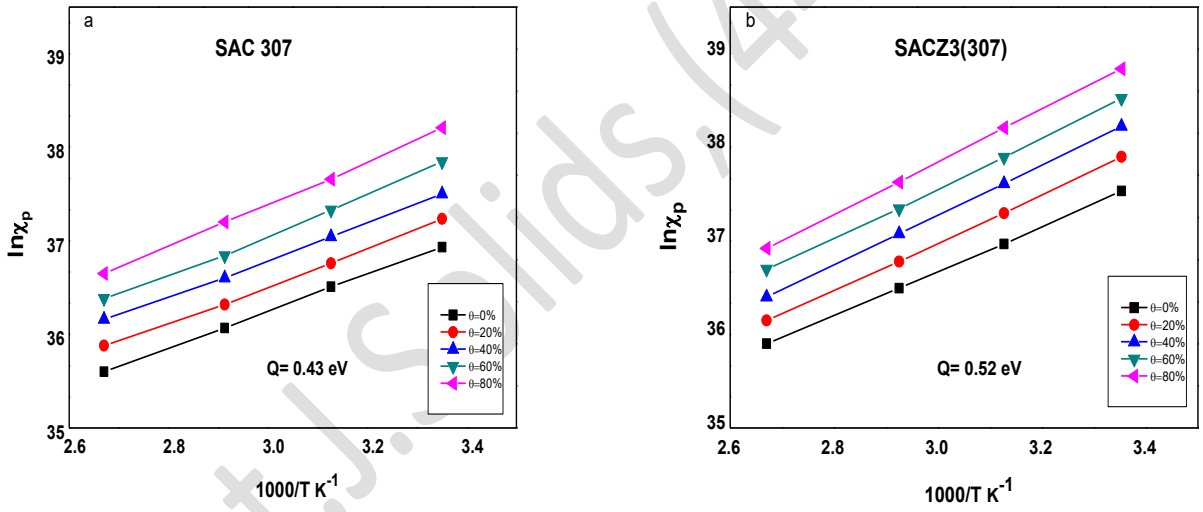

Fig.13. Relation between ln χ_p and 1000/T(K^{-1}) for : (a) SAC307and (b) SACZ3(307).

The average values obtained for the activation energies are 0.43 and 0.52 eV for SAC(307) and SACZ3(307) alloys, respectively. These values were found close to that previously reported [16, 28, 29] for the dislocation of intermetallic compound particles interaction. The Q value of both alloys indicates that they have the same rate-controlling mechanism.

4. Conclusions

The microstructure study showed that the addition of ZnO nanoparticles, Ag_3Sn and Cu_6Sn_5 IMCs were formed in a fine form distributed uniformly in the β-Sn matrix phase. The increase of pre-deformation by torsion resulted in an increase of $\boldsymbol{\sigma_{y0.2}}$,$\boldsymbol{\sigma_f}$ and χ_p while the fracture strain $\boldsymbol{\varepsilon_f}$ was found to behave differently. It decreased with increasing working temperature in SAC(307) for all degrees of deformation while it increased with working temperature for SACZ3(307) solder alloy. For the two investigated alloys, the deformation process was dominant by dislocation intermetallic compound particles interaction according to the obtained activation energies.

Conflict of interest

The author declared no potential conflicts of interest concerning the research, authorship, and/or publication of this article.

References

[1] M. Sobhy, M. A. Mahmoud, S. A. Fayek, J. A. Fawzy, A. Fawzy, G. Saad, Improved microstructure, thermal and tensile properties of Zn and graphene oxide nanosheets (GONSs) doped Sn–1 wt%Ag–0.5 wt%Cu for electronic assemblies, J Mater Sci: Mater Electron 28 (2017) 19181–19192. DOI:10.1007/s10854-017-7877-3

[2] M. M. Mansour, A. Fawzy, L. A. Wahab, G. Saad, Tensile characteristics of Sn–5wt%Sb–1.5wt%Ag reinforced by nanosized ZnO particles, Journal of Materials Science: Materials in Electronics 30(2019) 4831 https://doi.org/10.1007/s10854-019-00777-4

[3] A.B. El Basaty, A.M. Deghady, E.A. Eid, Influence of Small Addition of Antimony (Sb) on Thermal Behavior, Microstructural and Tensile Properties of Sn-9.0Zn-0.5Al Pb-Free Solder Alloy Mater. Sci. Eng. A 701 (2017) 245–253 https://doi.org/10.1016/j.msea.2017.06.092

[4] M. M. Mansour, G. Saad, L. A. Wahab, A. Fawzy, Indentation creep behavior of thermally aged Sn-5wt%Sb-1.5wt%Ag solder integrated with ZnO nanoparticles, Journal of Materials Science: Materials in Electronics,30(2019) 8348 DOI:10.1007/s10854-019-01152-z

[5] A. Fawzy, S.A. Fayek, M. Sobhy, E. Nassr, M.M. Mousa, G. Saad, Tensile creep characteristics of Sn–3.5Ag–0.5Cu (SAC355) solder reinforced with nano-metric ZnO particles, Materials Science & Engineering A 603 (2014)1–10. DOI:10.1016/j.msea.2014.02.061

[6] A. Fawzy, S. A. Fayek, M. Sobhy, E. Nassr, M. M. Mousa, G. Saad, Effect of ZnO nanoparticles addition on thermal, microstructure and tensile properties of Sn–3.5 Ag–0.5 Cu (SAC355) solder alloy, J Mater Sci: Mater Electron 24 (2013) 3210–3218 https://doi.org/10.1007/s10854-013-1230-2

[7] A.R. Geranmayeh, R. Mahmudi, Power law indentation creep of Sn-5% Sb solder alloy, J. Mater. Sci., 40 (2005) 3361. https://doi.org/10.1007/s10853-005-0421-5

[8] R. Mahmudi, S. Mahin-Shirazi, Effect of Sb addition on the tensile deformation behavior of lead-free Sn–3.5Ag solder alloy. Mater Des 32 (2011) 5027–5032. https://doi.org/10.1016/j.matdes.2011.05.052

[9] A.A .El-Daly, Y. Swim, A.E. Hammad. Influence of Ag and Au Additions on Structure and Tensile strength of Sn-5Sb Lead-free solder Alloy. J Mater Sci Technol, 24 (2008) 921–925. https://jmst.org/CN/Y2008/V24/I06/921

[10] A.A .El-Daly, Y. Swilem, A.E .Hammad. Creep properties of Sn–Sb-based lead-free solder alloys. J Alloys Compd 471(2009) 98-104. DOI:10.1016/j.jallcom.2008.03.097

[11] A.A. El-Daly, A.M. El-Taher, Evolution of thermal property and creep resistance of Ni and Zn-doped Sn–2.0Ag–0.5Cu lead-free solders, Materials and Design 51 (2013) 789–796. DOI:10.1016/j.matdes.2013.04.081

[12] L. Gao, S. Xue, L. Zhang , Z. Sheng , F. Ji, W. Dai , S. Yu a, G. Zeng, Effect of alloying elements on properties and microstructures of Sn-Ag-Cu solders, Microelectronic Engineering 87 (2010) 2025–2034. https://doi.org/10.1016/j.mee.2010.04.007

[13]. L.C. Tsao, S.Y. Chang, Effects of Nano-TiO_2 additions on thermal analysis, microstructure and tensile properties of Sn3.5Ag0.25Cu solder Mater. Design 31 (2010) 990- 993. https://doi.org/10.1016/j.matdes.2009.08.008

[14] J.Wang , L.Ma, T.wang, F.Guo, Effect of SiC nanoparticles on SACX305-TSV reliability under thermal load . Journal of Materials Science 57 (2022)1621-1632.DOIhttps://doi.org/10.1007/s10853-021-06821-1

[15] K.S.Kim , S.H.Huh ,K.Suganuma ,,"effect of fourth alloying additives on microstructures and tensile properties of Sn-Ag-Cu alloy and Joints with Cu , Microelectronics reliability 43 (2003)259-267. doi:10.1016/s0026-2714 (02)00239-1

[16] M.A. Mahmoud, A.F. Abd El-Rehim, M. Sobhy, R.M. Abdel Rahman,

Effect of torsional oscillations on the stress–strain behavior of Al–5 wt% Mg alloy. Materials Science and Engineering A 528 (2011) 6026. DOI:10.1016/J.MSEA.2011.04.061

[17] L.C. Tsao, S.Y. Chang, C.I. Lee, W.H. Sun, C.H. Huang, Effects of nano-Al_2O_3 additions on microstructure development and hardness of Sn3.5Ag0.5Cu solder Materials &Design 31 (2010) 4831-4835. https://doi.org/10.1016/j.matdes.2010.04.033

[18] Y. Shi, J. Liu, Z. Xia, Y. Lei, F. Guo, X. Li, Creep property of composite solders reinforced by nano-sized particles J. Mater. Sci. Mater. El 19 (2008) 349-356. DOI:10.1007/s10854-007-9327-0

[19] P. Liu, P. Yao, J. Liu, Effect of SiC Nanoparticle Additions on Microstructure and Microhardness of Sn-Ag-Cu Solder Alloy, J. Electron. Mater. 37 (2008) 874-879. https://doi.org/10.1007/s11664-007-0366-3

[20] J. Shen, Y.C. Chan, Effects of ZrO_2 nanoparticles on the mechanical properties of Sn–Zn solder joints on Au/Ni/Cu pads J. Alloy. Compd. 477(2009)552-559. DOI:10.1016/j.jallcom.2008.10.140

[21] A.K. Gain, Y.C. Chan, W.K.C. Yung, Microstructure, thermal analysis and hardness of a Sn–Ag–Cu–1 wt% nano-TiO_2 composite solder on flexible ball grid array substrates Microelectronics Reliability, 51 (2011)975-984. DOI:10.1016/j.microrel.2011.01.006

[22] I.E. Anderson, J.C. Foley, B.A. Cook, J. Harringa, R.L. Terpstra, O. Unal, Alloying effects in near-eutectic Sn-Ag-Cu solder alloys for improved microstructural stability

J. Electron. Mater. 30 (2001) 1050-1059. https://doi.org/10.1007/s11664-001-0129-5

[23] A. Fawzy, Effect of Zn addition, strain rate and deformation temperature on the tensile properties of Sn–3.3 wt.% Ag solder alloy Materials Characterization 58 (2007) 323- 331.

https://doi.org/10.1016/j.matchar.2006.05.013

[24] N. F. Mott: Dislocations and Mechanical Properties of Crystals, New York; J.Wiley (1957) 548.

[25] M.Koiwa and R.R. Hastiguti: Trans. Japan Inst. Metals 81 (1976) 75.

[26] M.A.Kenawy, G.Saad , M.T.Mostafa .The effect of pre-torsional deformation on creep properties of tin 0.5 at.% bismuth alloy Solid State comm.46(1983)763- 767.

https://doi.org/10.1016/0038-1098(85)91114-7

[27] A.M. Abd el-khalek, Effect of grain size and Indium addition on tensile characteristics of Al–1Si alloy Mater. Sci. Technol. 24 (2013) 1333-1339.
https://doi.org/10.1179/174328407X213125

[28] J. Jiang, J.E. Lee, K.S. Kim, K. Suganuma, Oxidation behavior of Sn–Zn solders under high-temperature and high-humidity conditions J. Alloy. Comp. 462 (2008) 244-251.

DOI: 10.1016/j.jallcom.2007.08.007

[29] M.J. Esfandyarpour, R. Mahmudi, Microstructure and tensile behavior of Sn–5Sb lead-free solder alloy containing Bi and Cu Mat. Sci. Eng. A-Struct. 530 (2011) 402-410. DOI10.1016/j.msea.2011.09.103